Marine Geodesy, 26: 399–421, 2003

ISSN: 0149-0419 print / 1521-060X online
DOI: 10.1080/01490410390256727

Taylor & Francis
Taylor & Francis Group

The 1-Centimeter Orbit: Jason-1 Precision Orbit Determination Using GPS, SLR, DORIS, and Altimeter Data

S. B. LUTHCKE

NASA Goddard Space Flight Center
Laboratory for Terrestrial Physics
Space Geodesy Branch
Greenbelt, Maryland, USA

N. P. ZELENSKY

Geodynamics Group
Raytheon ITSS
Lanham, Maryland, USA

D. D. ROWLANDS
F. G. LEMOINE

NASA Goddard Space Flight Center
Laboratory for Terrestrial Physics
Space Geodesy Branch
Greenbelt, Maryland, USA

T. A. WILLIAMS

Geodynamics Group
Raytheon ITSS
Lanham, Maryland, USA

The Jason-1 radar altimeter satellite, launched on December 7, 2001 is the follow on to the highly successful TOPEX/Poseidon (T/P) mission and will continue the time series of centimeter level ocean topography measurements. Orbit error is a major component in the overall error budget of all altimeter satellite missions. Jason-1 is no exception and has set a 1-cm radial orbit accuracy goal, which represents a factor of two improvement over what is currently being achieved for T/P. The challenge to precision orbit determination (POD) is both achieving the 1-cm radial orbit accuracy and evaluating the performance of the 1-cm orbit. There is reason to hope such an improvement is possible. The early years of T/P showed that GPS tracking data collected by an on-board receiver holds great promise for precise orbit determination. In the years following the T/P launch there have

Received 13 June 2003; accepted 1 August 2003.

The authors wish to thank Bruce Haines for the JPL GPS APC map and discussions on the Jason-1 BlackJack GPS receiver. The authors also wish to thank Jean Paul Berthias and the CNES POD team for the prelaunch satellite characteristic definitions and models, and for distribution and assistance with supporting Jason-1 data. The authors thank John Ries for his collaboration on validating the initial Jason-1 SLR and DORIS modeling details. The authors acknowledge the NASA physical oceanography program and the TOPEX/Poseidon project for their support.

Address correspondence to Scott B. Luthcke, Space Geodesy Branch, Code 926, NASA Goddard Space Flight Center, Greenbelt, MD 20771, USA. Email: Scott.B.Luthcke@nasa.gov

been several enhancements to GPS, improving its POD capability. In addition, Jason-1 carries aboard an enhanced GPS receiver and significantly improved SLR and DORIS tracking systems along with the altimeter itself. In this article we demonstrate the 1-cm radial orbit accuracy goal has been achieved using GPS data alone in a reduced dynamic solution. It is also shown that adding SLR data to the GPS-based solutions improves the orbits even further. In order to assess the performance of these orbits it is necessary to process all of the available tracking data (GPS, SLR, DORIS, and altimeter crossover differences) as either dependent or independent of the orbit solutions. It was also necessary to compute orbit solutions using various combinations of the four available tracking data in order to independently assess the orbit performance. Towards this end, we have greatly improved orbits determined solely from SLR+DORIS data by applying the reduced dynamic solution strategy. In addition, we have computed reduced dynamic orbits based on SLR, DORIS, and crossover data that are a significant improvement over the SLR- and DORIS-based dynamic solutions. These solutions provide the best performing orbits for independent validation of the GPS-based reduced dynamic orbits. The application of the 1-cm orbit will significantly improve the resolution of the altimeter measurement, making possible further strides in radar altimeter remote sensing.

Keywords precison orbit determination, satellite altimetry, remote sensing

The joint US/French Jason-1 satellite altimeter mission, launched on December 7, 2001, continues the time series of centimeter-level ocean topography observations as the follow-on to the highly successful TOPEX/Poseidon (T/P) radar altimeter satellite. Jason-1 orbits the Earth in a 1335 km altitude, near-circular orbit with a 66.03° inclination. Like any other altimeter satellite, the accurate knowledge of the history of the spacecraft center of mass location (the orbit) is critical to the overall success of the mission. Radial orbit errors directly map into the fundamental science observations, namely the altimeter-derived topographic height. In fact, the radial orbit error is a major component in the overall measurement error budget.

For T/P, the radial orbit error was the dominant component of the original prelaunch mission error budget accounting for over 12.5 cm of the overall 13.3 cm Root Sum Square (RSS) error (Tapley et al. 1994). Fortunately, significant advances in Precision Orbit Determination (POD) measurement and force modeling and solution methodology have allowed the current 2-cm level of T/P radial orbit accuracy to be achieved (Chelton et al. 2001; Marshall et al. 1995; Tapley et al. 1994). For more than a decade, these highly accurate orbits have been computed at the Space Geodesy Branch of Goddard Space Flight Center (GSFC) without interruption in delivery to the project. Part of the success of the T/P mission can be attributed to the remarkable improvement of the radial orbit accuracy over the original error budget and the continued delivery of these high accuracy orbits.

In order to continue the T/P standard of observations, Jason-1 has a radial orbit error budget requirement of 2.5 cm. However, being the follow-on to T/P, expectations are significantly higher and a 1.0-cm radial orbit accuracy goal has been set. Obtaining another factor of two improvement in orbit accuracy over that achieved for T/P certainly presents its challenges. Fortunately, Jason-1 POD can rely on four independent tracking data types, including near continuous tracking data from the dual frequency codeless BlackJack GPS receiver, Satellite Laser Ranging (SLR), Doppler Orbitography and Radiopositioning Integrated by Satellite (DORIS), and the altimeter range itself in the form of crossovers. Even more fortunate is the fact that each of the tracking data systems have been significantly upgraded over those used on T/P. Jason-1 benefits from an improved codeless BlackJack GPS receiver capable of acquiring carrier phase and pseudorange observations at both L1 and L2 frequencies regardless of antispoofing (AS) from up to 12 simultaneous GPS spacecraft (Haines et al. 2003a). The DORIS receiver is capable of tracking two ground beacons simultaneously, while T/P's DORIS receiver could only track one. Additionally, a 0.1 mm/s improvement (over T/P) in the noise characteristics of the Jason-1 DORIS receiver has been

observed as measured by our range rate DORIS residuals. Finally, the Jason-1 nine corner cube hemispherical Laser Retroreflector Array (LRA) represents a significant improvement over T/P's complex laser ring array (Marshall et al. 1995).

Because we do not have a measure of absolute orbit accuracy, much of the challenge in meeting the Jason-1 orbit accuracy goal is the performance assessment of candidate orbit solutions. As we will discuss, assessing orbit accuracy, determining the best orbit strategy, and characterizing the resultant orbit errors require the processing of all tracking data types whether they are included in the orbit solution or withheld as independent data to assess orbit performance. We have computed several high accuracy solutions from various combinations of tracking data and different solution strategies. These orbits are compared along with a detailed analysis of crossover constraint and SLR data performance in order to characterize and quantify orbit error. As will be shown, our best orbits are those computed from GPS data using a reduced dynamic technique. Although we do not have a direct measure of absolute orbit accuracy, the suite of analyses discussed in this article suggest our GPS-based reduced dynamic orbits likely achieve the 1-cm radial orbit accuracy goal. In order to characterize orbit error properly, we have also computed reduced dynamic orbits based on SLR, DORIS, and crossover data. Among the various orbit solutions we have computed, the reduced dynamic orbits determined from SLR, DORIS, and crossover data are closest in performance to our reduced dynamic GPS orbits and provide for a much better comparison than, for example, dynamic orbits based solely on SLR and DORIS tracking.

The purpose of this article is to address two major issues important to those interested in oceanographic studies from the analysis of the altimeter data: (1) which POD strategy, combination of tracking data, and solution technique produces the best orbits; and (2) what are the error characteristics of these orbits. This article does not discuss the various details of each tracking system, but focuses on the analysis of various orbit strategies and the resultant orbit errors. Details of the various tracking systems can be found in Chelton et al. (2001).

POD Methodology

Solution Strategy Overview

Among the key issues that comprise an orbit solution strategy for any satellite are: (1) arc length (i.e., time interval over which the solution will be made), (2) parameterization (including number and type of empirical parameters to be used), and (3) data use (editing, combination of data types, weighting). Of course, the orbit strategy for Jason-1 benefits greatly from the many years of experience from T/P. Arc length decisions for Jason-1 are based on the T/P experience. Orbit solutions that do not use GPS data are nominally made in arcs of 10 days. Orbit solutions that do use GPS data are made in shorter arcs (typically 30 h) and blended together to provide a consistent solution over a 10-day Jason-1 repeat cycle. The shorter arcs used in GPS-based solutions are a matter of computational convenience. The T/P experience demonstrated that the strength of the GPS data permits the use of daily arcs without degrading an orbit solution (Bertiger et al. 1994; Yunck et al. 1994).

The data use and parameterization issues for Jason-1 cannot be decided solely from the T/P experience. This is primarily due to an improvement in the GPS circumstances for Jason-1. First, as previously mentioned, the Jason-1 GPS receiver represents a significant enhancement over the receiver carried on T/P. Second, GPS data products (IGS orbits, station positions) and modeling have improved greatly since 1995 when the policy of AS significantly degraded the quality of T/P GPS data. The concept of reduced dynamic parameterizations for GPS-based orbit solutions was validated for T/P (Bertiger et al. 1994; Yunck et al. 1994). Of course, the concept of reduced dynamics still applies for Jason-1, but

the specifics of the parameterization requires reexamination given the improved GPS circumstances. In addition, the GPS improvements require a reexamination of data weighting issues in solutions that use GPS data together with other data types.

All of our Jason-1 orbit solutions, whether standard dynamic or reduced dynamic, use empirical acceleration parameters. The standard T/P SLR+DORIS orbit solutions that are placed on the mission GDRs use one cycle per revolution (1-cpr) empirical orbit acceleration parameters (Colombo 1989). These 1-cpr accelerations are formulated as:

$$\begin{aligned} acceleration &= A\cos(\omega t) + B\sin(\omega t) \\ \omega &= 2\pi / T \\ T &\equiv orbital\ period, \end{aligned} \tag{1}$$

where A and B terms are estimated in the along- and cross-track directions (the along-track accelerations affect both the along-track and the radial components of the orbit). These A and B parameters are valid over a certain interval (in the standard dynamic T/P orbit solutions, the interval is one day). When these A and B terms are recovered over multiple intervals, force model error is characterized and accommodated as a once per revolution phenomenon with slowly varying phase and amplitude. An important aspect of the Jason-1 orbit solution strategy is the determination of the optimal length interval for these A and B parameters. This is related to the topic of reduced dynamics.

Reduced Dynamic Solutions

The concept of reduced dynamics is not very sharply defined. In general, reduced dynamic orbits use a large number of empirical accelerations. These acceleration parameters are usually (but not always) constrained. Dense geometrically strong tracking data such as GPS make reduced dynamic solutions possible. However, it has been our experience that even GPS-based orbit solutions do not benefit from the use of empirical accelerations with suborbital intervals unless the empirical accelerations are tied together with time correlation constraints as in Rowlands et al. (1997). Our time correlation constraint equations give a least squares batch orbit solution the same advantages that time-correlated parameters can give to a Kalman-filter–based solution. Along with the determination of the optimal acceleration interval the optimal use of time correlation constraint equations is a key aspect of our Jason-1 orbit solution strategy.

The time correlation constraint equations require two pieces of information, a correlation time and a standard deviation. For example, the A parameters (Equation (1)) from two acceleration intervals that differ by a time, T, will be constrained to be equal with a weight (WT) formulated as

$$\begin{aligned} WT &= \frac{1}{\sigma^2} e^{1-\frac{T}{CT}} \\ \sigma &\equiv correlation\ sigma \\ CT &\equiv correlation\ time. \end{aligned} \tag{2}$$

For the purposes of discussion, a dynamic orbit solution is the special case of a reduced dynamic orbit solution where the correlation sigma is very large. When searching for an optimal parameterization, it is useful to look at dynamic and reduced dynamic parameterizations as different ends of the same continuous spectrum of possible orbit solutions.

Our tuning procedure begins its search for an optimal parameterization at the dynamic end of the spectrum and proceeds by gradually decreasing the interval associated with the

empirical accelerations. In the beginning of the search as the interval is decreased, performance of the orbit solution generally improves (orbit solution metrics will be discussed below). However, at some point the solutions will begin to degrade as the interval is decreased. This critical interval can be made smaller (optimization can be pursued further) by beginning to use time correlation constraint equations (increasing the weight of these equations to a significant level). At this point in the search we begin to optimize a solution by increasing the effect of constraints (decreasing the sigma and increasing the correlation time). After the optimal use of constraints is found for a given acceleration interval, a smaller interval is pursued. Eventually the interval becomes small enough so that constraint information does not improve solution performance.

The use of the various tracking data types is very much a consideration in tuning a parameterization for an orbit solution. We have access to four tracking data types (GPS, SLR, DORIS, and radar altimetry in the form of crossover constraints). It is important to note that we use Double Differenced LC phase observations (DDLC) as our GPS tracking data. Our GEODYN software can use any of the four Jason-1 data types individually or in combination to form the normal equations for an orbit solution. However, at the beginning of the tuning procedure, we prefer to form normal equations using only the minimum number of data types required to obtain a good solution. For some solutions we start using only GPS data, for others we start by combining only DORIS and SLR data. The fit of the withheld data types of an orbit solution is a strong indicator of orbit quality, at least in the relative sense (as a discriminator between two candidate solutions). For example, when tuning a GPS-based solution, withheld SLR data are an important indicator of solution quality. GPS orbit solutions rely on the use of thousands of ambiguity bias parameters while modeling SLR in general does not require bias estimation except for a handful of stations. The SLR data provides an unambiguous measure of orbit performance. The withheld SLR data were invaluable in determining the optimal measurement model and reduced dynamic parameterization. Although withheld SLR data provide the best possible metric, altimeter crossovers are also useful as a withheld data type. To a lesser extent, orbit overlap statistics (consistency of two adjacent arcs in a common time interval) and the fit of the data used in the solution are also used to measure orbit solution performance.

Candidate Solutions and Combining Data Types

After GPS only or SLR+DORIS orbit solutions are tuned, we proceed to the addition of other data types to these basic solutions. The optimal relative weighting of the data types is tuned in the same manner as the optimal parameterization discussed above, using withheld data, orbit overlaps, and data included in the solutions as performance metrics.

In selecting orbit solution strategies, we sought to determine the best orbit and then to characterize the orbit error. In order to properly characterize orbit error, it is important to compare two orbits of near equal performance determined from independent tracking. In this article we discuss our analysis from five candidate orbit solution strategies that run the spectrum of data combination and parameterization: (1) SLR and DORIS dynamic (SLR+DORIS Dyn); (2) SLR and DORIS reduced dynamic (SLR+DORIS RD); (3) SLR, DORIS and crossover reduced dynamic (SLR+DORIS+Xover RD); (4) GPS reduced dynamic (GPS RD); and (5) GPS and SLR reduced dynamic (GPS+SLR RD). It is important to note that we have also analyzed solutions determined from GPS+SLR+DORIS data. From our initial analysis, these solutions did not show improved performance over our GPS-only or GPS+SLR-based solutions. The analysis presented in this article shows the DORIS residuals change little or not at all among our five candidate solutions. Additionally, the DORIS performance has been linearly degrading over time. It is believed that the problem is due to increasingly erratic Jason-1 clock behavior as it periodically passes through the

South Atlantic magnetic anomaly (Willis et al. 2003). This problem and the means around it are being investigated. Because of these reasons and the fact that the GPS+SLR+DORIS solutions do not contribute to our suite of independent orbits, we have chosen not to pursue this solution strategy further within this article. However, it is important to mention that the DORIS data are invaluable in our SLR+DORIS dynamic and reduced dynamic solutions. The DORIS data provides the necessary temporal and spatial coverage to support reduced dynamic solutions when the GPS data are not used.

POD Details

The details of our POD solutions are too numerous to discuss at length in this article. Therefore, these details have been summarized in Tables 1 and 2. However, there are a few specific issues that warrant a limited discussion here. Much of the following discussion is focused on GPS measurement modeling details. These details are especially important for our GPS RD solutions, because the reduced dynamic solution technique is most susceptible to measurement modeling errors.

We use a consistent set of ITRF2000 SLR, DORIS, and GPS station positions with few modifications and corrections (Altamimi et al. 2002). Our GPS stations were selected based on International GPS Service (IGS) reported performance and their global distribution. Our GPS solutions use IGS final orbits for the GPS satellite positioning. However, we have found it necessary to edit these reported orbits because, on any given day, a few of these orbits can possess several decimeters of error. Our procedure for editing these orbits starts with using the IGS orbits as Earth Centered Fixed (ECF) x, y, and z tracking data. We then determine orbits for each of the GPS satellites using the ECF position tracking data and a very aggressive reduced dynamic solution strategy. These orbit solutions are made using overlapping (by 6-h) 30-h arcs. The 30-h arcs are constructed from one day of IGS orbits and 6-hrs. of the next day. This is important for checking the GPS orbit consistency. Typically, the fit to the IGS orbits is on the order of 1-cm. For poorly performing IGS GPS orbits the fit is greater than 4–5 cm. We also make overlap orbit comparisons from our GPS orbit solutions determined using the IGS position data. Typically these orbit overlaps are at the 0.5–2.5 cm radial RMS level. However, for poorly performing IGS GPS orbits radial orbit overlaps can be as large as 60 cm or greater. Using both of these tests we track the performance of the IGS orbits for all of the days we are interested in producing LEO orbits. Trends are easily observed, and the poor-performing IGS GPS orbits can be edited. Typically 0–2 satellites are edited per day, but on occasion as many as five have been edited. There are several reasons for the poor performing orbits, including reaction wheel problems, autonomous momentum dumps, solar array slewing, and small firings of the thrusters due to sunlight sensor interference at eclipse entrance and exit. For example, GPS satellites SVN/PRN 15/15 and 17/17 typically have poor-performing IGS orbits. These GPS satellites are rapidly approaching the end of operations and have serious problems such as reaction wheel problems during eclipse.

Proper modeling of the GPS antenna phase center is extremely important to the overall performance of the GPS-based solutions. During the initial analysis of the GPS data we determined that there was a significant difference in the z-component (zenith) of the Jason-1 GPS antenna phase center offset from the a priori value (z-component delta). To make matters worse the z-component delta showed a significant difference between fixed (~ -4 cm) and sinusoidal yaw steering (~ -6 cm) attitude modes of the spacecraft. Researchers at JPL then computed an antenna phase center map (APC map) from postfit GPS undifferenced LC residuals (Haines et al. 2003b). They used approximately one year of data and averaged the residuals into a map with 2° resolution in elevation and 5° resolution in azimuth referenced to the antenna frame. The map significantly improves GPS-based orbit

TABLE 1 POD Summary(1): Models, Data, and Parameters

Geophysical models and parameters	
Gravity/Tides	JGM3 (Tapley et al. 1994)/GOT99.2 (Ray 1999)
Atmospheric density	MSIS-86 (Hedin 1988)
Station coordinates	ITRF2000
Earth orientation	IERS C 04
Planetary ephemeris	DE403
Tracking data	
GPS	• Double-differenced, ionosphere-free combination of L1 and L2 carrier phase (DDLC). • ∼33 IGS stations (best performing/optimal distribution)
SLR / DORIS/ altimeter crossovers	DORIS "SAA" station data included; light editing of altimeter crossover data
Modeling	
Jason-1	• GSFC antenna LC phase correction (APC) map • a priori GPS antenna LC phase center offset in S/C Body Fixed (SBF): ○ (SBF X, Y, Z); (2.389, −0.218, −0.504) (m) • estimated SLR offset in SBF: ○ (SBF X, Y, Z); (1.158, 0.598, 0.6828) (m) • a priori DORIS offset in SBF: ○ (SBF X, Y, Z); (1.171, −0.598, 1.027) (m) • a priori center of mass offset in SBF: ○ (SBF X, Y, Z); (0.942, 0.000, 0.000) (m) • GPS antenna orientation unit vectors in SBF: ○ Boresite (SBF X, Y, Z); (0.498, −0.044, −0.866) ○ X Dipole (SBF X, Y, Z); (0.867, 0.025, 0.497) • SLR retro-reflector range correction: −0.049 m • s/c orientation: ○ telemetered quaternions (attitude model as needed) • s/c area and solar radiation pressure: prelaunch "Box-wing" model[1]
GPS satellites	• IGS final/precise GPS ephemerides-Edited • IGS Block II, IIA, IIR phase center of mass offsets • New GPS satellite attitude (Bar-Sever 1996)
GPS stations	Antenna phase center
SLR/DORIS/GPS	Troposphere refraction
GPS	• Outlier editing/cycle slip detection and correction • Phase wind-up • GPS receiver preprocess clock correction for 2nd order effect

[1]CNES POD Team—http://calVAL.jason.oceanobs.com/html/calval_plan/poe/models_jason.html.

TABLE 2 POD Summary (2): Data Weighting, Estimated Parameters, and Arc Length

Data Weighting		
Data sigma weighting	SLR/DORIS dynamic:	10 cm SLR; 2 mm/s DORIS
	SLR/DORIS reduced Dynamic:	10 cm SLR; 1 mm/s DORIS
	SLR/DORIS/crossover reduced dynamic:	10 cm SLR; 1 mm/s DORIS; 10 cm crossover
	SLR/GPS reduced dynamic:	10 cm SLR; 10 cm GPS
Estimated parameters		
Measurement model	• GPS carrier phase ambiguity per pass • GPS troposphere scale factor every 60 min/station • DORIS measurement bias and troposphere scale factor per pass	
Force model	• SLR/DORIS-based solution dynamic parameterization: ○ State (pos. and vel.); C_D/ 8 h; Alg and Crs 1-cpr accelerations/24 h • SLR/DORIS-based solution reduced dynamic parameterization: ○ State (pos. and vel.); C_D/ 24 h; Alg and Crs 1-cpr accelerations/28 min; 45 min correlation time; 1.e-9 m/s^2 sigma • GPS-based solution reduced dynamic parameterization: ○ State (pos. and vel.); C_D/ 30 h; Alg and Crs 1-cpr accelerations/30 min; 60 min correlation time; 1.e-9 m/s^2 sigma • GPS/SLR-based solution reduced dynamic parameterization: ○ State (pos. and vel.); C_D/ 30 h; Alg and Crs 1-cpr accelerations/30 min; 60 min correlation time; 5.e-9 m/s^2 sigma	
Arc length/details		
Short arcs	GPS orbit solutions computed in 30-h arcs with 6-h overlapping time periods. The arcs do not necessarily start on 0 h of a day, but are constructed such that 10 short arcs evenly cover a Jason-1 repeat cycle.	
Long arcs	A long arc covers a Jason-1 10-day repeat cycle. SLR/DORIS solutions are computed over 10-day arcs. GPS long arcs are "blended" together from the center 24 h of 10 short arcs.	

solutions and removes the need for any correction to the a priori antenna phase center offset, much less a change in correction between attitude regimes.

At GSFC we have also computed our own APC map using a completely independent technique and software. We have developed our APC map by making a formal solution estimating parameters which describe the correction at each point on a $5^\circ \times 5^\circ$ grid in azimuth and elevation. The solution is determined using data from only twelve 30-h arcs carefully selected to sample all attitude regimes from day of year (DOY) 84 to DOY 223 of 2002. The correction parameters (common to all 12 arcs) are estimated simultaneously with the standard OD parameters from the 12 arcs. Table 3 shows the performance of the

TABLE 3 APC Map Performance in GPS RD Solutions: Residual Summary for Cycles 8–24

APC map	GPS DDLC RMS (cm)	Independent SLR RMS (cm)	Independent Xover RMS (cm)
No APC map	0.942	2.308	5.843
JPL APC map	0.758	1.704	5.767
GSFC APC map	0.752	1.701	5.766

GSFC and JPL maps compared to using no map. In the case where no map is used, the optimal attitude regime varying average phase center offsets have been applied. Both maps are a significant improvement over using no map with the varying offset correction. It is important to note that 93% of the these test data are independent from the GSFC APC map solution while 100% of these data were used in the JPL map development. Figure 1 shows the improvement in independent (not in the orbit solution) SLR residuals (all residuals not just high elevation) obtained using the GSFC APC map. The independent SLR residuals in Figure 1 have been fit to GPS RD solutions using the GSFC APC map and to no map using the varying offset correction. There is general improvement over the entire time series, but dramatic improvement in the fixed yaw attitude regimes is observed.

Figure 2 shows a comparison of the GSFC and JPL APC maps. The maps are very similar in the top quadrants, both capturing the same general features. However, the maps differ in the lower quadrants (about 0°). The reason for this is that our map is determined as

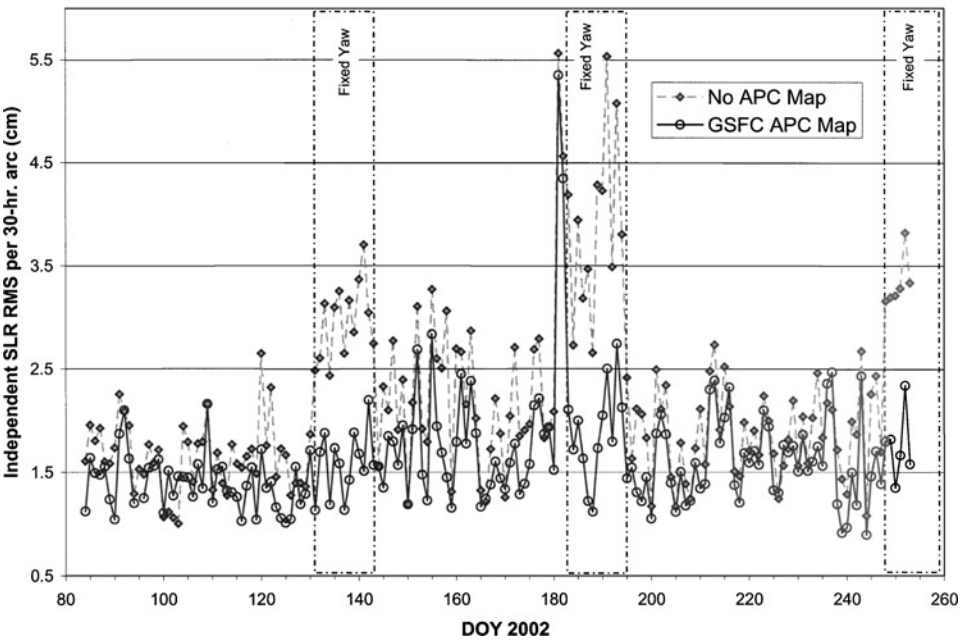

FIGURE 1 SLR residual test performance of GPS APC map. Accurate modeling of the GPS antenna phase center is required for POD. The time series of independent SLR residuals RMS/30-h arc, cycles 8–24, show the benefit of using the GSFC APC map correction. This is especially evident over the fixed-yaw regime. The "No APC Map" phase center offsets had been adjusted from the prelaunch values and represent our best solution short of using the APC map.

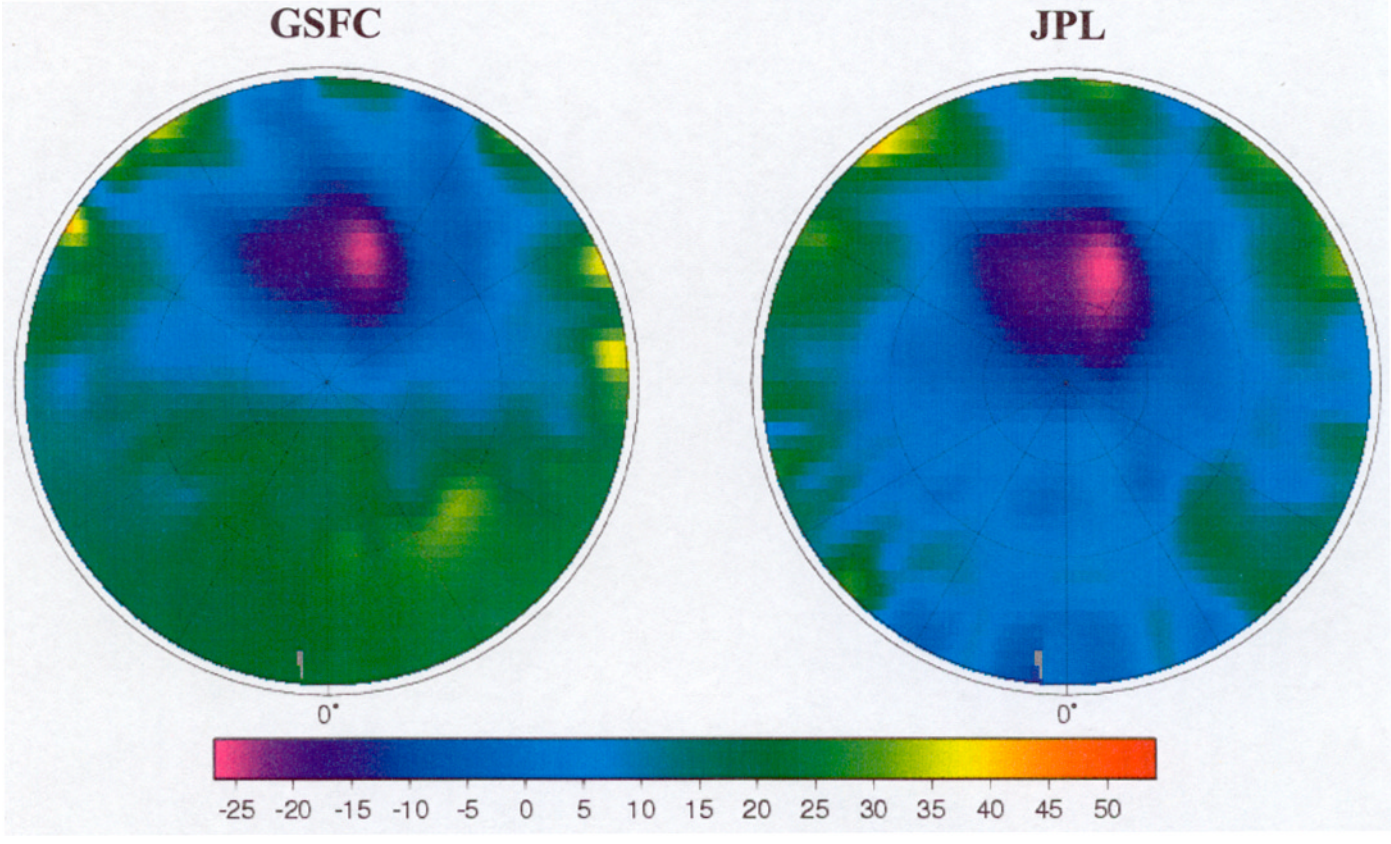

FIGURE 2 GPS antenna phase center maps (mm; azimuth clockwise; 0° to 90° elevation from outside to center) The APC map estimated postlaunch with GPS tracking data, is very important to POD. The 5° × 5° azimuth/elevation GSFC map was estimated in a formal solution using twelve 30-h arcs sampled over a β, cycle, and for which low elevation GPS double-difference phase data was edited. The JPL map (Haines et al. 2003b) was computed averaging one year of undifferenced GPS phase residuals into 5° × 2° azimuth/elevation bins.

part of the POD process after data editing. In our nominal POD processing, we edit data that are at low elevation with respect to the satellite local horizon. Because the Jason-1 GPS antenna is "tilted" $\sim 30^\circ$ from the zenith towards the spacecraft X (or the antenna 0°), our nominal data editing removes data in the lower antenna quadrants (about 0°). This does not adversely affect the resultant orbit solutions because the antenna model is well represented where the data are considered viable. The important point is that the antenna phase center maps determined from different software, data, and techniques give very similar results. This lends confidence that these maps can and should be estimated postlaunch. Also, our analysis shows that only a few days (twelve 30-h arcs) of data are necessary to determine the GPS APC map.

As in the case of the GPS, proper modeling of the SLR tracking point offset is very important. We model the Laser Retroreflector Array (LRA) optical center with respect to the spacecraft center of mass (CoM) as the difference of the vector from the SBF origin to the LRA tracking point (LRA offset) and the vector from the SBF to the CoM. The LRA consists of nine corner cubes arranged hemispherically and is expected to have a stationary optical center with a small constant bias. Therefore, an additional common range correction is applied to account for the optical center offset with respect to the LRA tracking point offset. To ensure precise modeling of the SLR observations, the LRA tracking point offset was adjusted in a formal least-squares solution using cycles 1–20 of Jason-1 SLR tracking data. The new LRA offset improves the SLR model and the POD as evidenced by the reduction of the SLR residuals over dependant and independent cycles of data (see Table 4). Adjustment of the LRA offset is largely in the X component (Z is along boresite of altimeter, Y is along solar array axis of rotation, and X completes the right-handed orthogonal system), and may compensate for errors in modeling the offset, CoM, and optical center correction. Previous analysis has shown that the LRA adjustment in X agrees with that of the GPS phase center adjustment in X suggesting a common CoM offset. However, as discussed above, we are currently absorbing any mean offset error in our GPS APC map. Therefore, we apply the LRA offset correction as such and not as a common CoM offset correction.

Quantifying and Characterizing Orbit Error

Although the challenge of centimeter-level POD is to quantify and characterize the orbit error, no direct measure of absolute orbit error exists. Therefore, we must use several different performance tests to help us gauge and understand the orbit error contained in the POD solutions. These orbit tests rely on the processing and analysis of all tracking data types available along with multiple solution techniques. Tracking data postfit residual performance is an important performance metric. Both dependent (used in the orbit solution) and independent (withheld from the orbit solution) data residual performance are assessed. The independent data residuals are an important discriminator of solution performance,

TABLE 4 Summary of LRA Offset Analysis

	LRA offset spacecraft body-fixed coordinates (cm)			SLR residuals over cycles (cm) 1–20		SLR residuals (cm) over cycles 21–25 (independent data)	
Description	X	Y	Z	Mean	RMS	Mean	RMS
a-priori	117.1	59.8	68.28	−0.060	1.897	−0.214	1.799
Estimated LRA offset	115.8	59.8	68.58	+0.049	1.835	−0.130	1.721
Formal sigma	0.10	0.10	0.06				

TABLE 5 Independent and Dependent Data Residual Summary for Cycles 8–24

Solution type	GPS DDLC RMS (cm)	DORIS RMS (mm/s)	SLR RMS (cm)	Xover RMS (cm)	Xover mean (cm)
SLR+DORIS Dyn.		0.420	1.706	*5.928*	*0.229*
SLR+DORIS RD		0.418	1.734	*5.868*	*0.219*
SLR+DORIS+ Xover RD		0.418	1.914	5.780	0.049
GPS RD	0.75	*0.420*	*1.701*	*5.766*	*−0.029*
GPS+SLR RD	0.77	*0.420*	1.342	*5.752*	*−0.029*

and in the case of high-elevation SLR residuals, provide an important measurement of radial orbit error. Orbit overlap tests (consistency of two adjacent arcs in a common time interval) are also used to assess the solution precision as a necessary but not sufficient condition for 1-cm radial orbit accuracy. An important means of characterizing orbit error is to compare ephemerides computed from independent tracking data. However, the orbits compared should be as close to equal quality as possible, otherwise the less accurate orbit dominates the difference**.** The detailed analysis of altimeter crossover residuals is another important tool for characterizing orbit error.

Tracking Data Residual and Orbit Overlap Analysis

Tracking data residual performance is used as a first step in understanding the relative performance of our candidate solutions. Table 5 presents the tracking data residual performance statistics accumulated over repeat cycles 8 through 24. Both dependent and independent (shown in italics) residual statistics are shown. Using the altimeter crossover residuals as the primary discriminator, we can see that the reduced dynamic technique has improved the SLR+DORIS solution. The SLR+DORIS RD solutions rely more heavily on the DORIS data, due to their better temporal and spatial coverage over SLR tracking. This can be seen from the SLR+DORIS RD solution's reduction in DORIS data fit and slight increase in the SLR fit over the SLR+DORIS Dyn solution fits. As would be expected, still further improvement in crossover data fit, at the expense of SLR data fit, is observed when adding crossover data to the SLR+DORIS RD solution. Orbits computed solely from GPS tracking data with a reduced dynamic technique (GPS RD) have better crossover and SLR fits than any of the solutions performed without GPS data. This is especially remarkable because the SLR and crossover data have been withheld from the GPS RD orbit solutions. Still further improvement in independent crossover data fits are obtained with GPS RD solutions that include SLR data in the orbit determination. Although the SLR data is not independent to the GPS+SLR RD solutions, we do observe a stunning improvement in the SLR fits over any other solution that does not use GPS data.

The tracking data residual summary presented in Table 5 clearly shows the GPS-based reduced dynamic solutions represent a significant improvement over any orbit solution relying solely on SLR and DORIS tracking data. The GPS RD solution improvement in crossover RMS over SLR+DORIS Dyn represents 1.38 cm RMS in radial orbit accuracy improvement and 1.09-cm RMS radial orbit improvement over the SLR+DORIS RD solution. Adding SLR data to our GPS RD solutions is a still further 0.40-cm RMS radial orbit improvement as indicated by the independent altimeter crossover residual statistics. The tracking data analysis presented in Table 5 shows the best orbits are GPS-based orbits computed using a reduced dynamic technique. These GPS-based reduced dynamic orbits

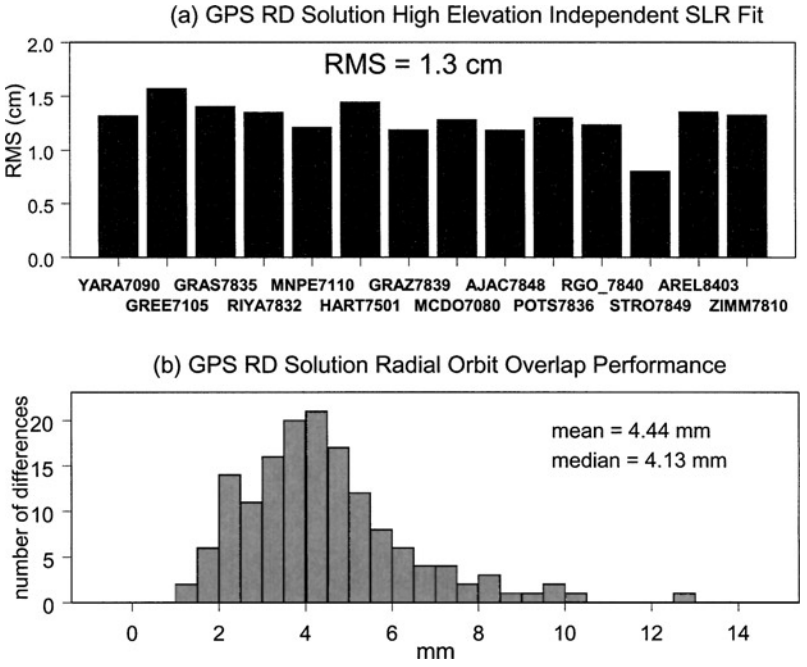

FIGURE 3 GPS RD (a) high elevation independent SLR fit and (b) radial orbit overlap performance. (a) Measurement biases estimated from high elevation pass SLR residuals offer the best single metric to gauge radial orbit accuracy. The RMS of the estimated biases indicates orbit error does not exceed 1.3 cm. The actual radial error is less because the statistic contains other error sources as well. SLR data above 60 degrees are selected for the high elevation test. (b) Histogram of the radial orbit overlap difference RMS for each 6-h overlapping time period between GPS RD 30-h arcs from cycle 8–24. The result indicates the GPS reduced dynamic solutions are consistent to 4 mm.

represent a significant improvement over the SLR+DORIS Dyn. orbits considered to be accurate at the ∼2 cm radial RMS level.

The most direct measurement of radial orbit accuracy is obtained from high elevation SLR pass biases. A pass bias is estimated for independent SLR data that exceeds 60° in elevation. The data from historically well performing SLR stations that have acquired at least 10 high elevation passes were used. For each of these stations the RMS of the pass biases is computed and an overall RMS is also computed. Figure 3a shows the GPS RD solution independent high elevation SLR pass bias RMS for each station. It is important to note that while this is one of the most direct means for measuring radial orbit accuracy, it is not a perfect test and contains error sources other than radial orbit error (e.g., station position, LRA offset, and a small horizontal orbit error component). With this in mind, the high elevation SLR analysis indicates the GPS RD orbit solutions have a radial orbit accuracy better than 1.3 cm. It is also important to note the consistency in performance across stations shown in Figure 3a. Orbit accuracy can only be as good as orbit solution precision. We can quantify this accuracy limit using orbit overlap tests to determine the precision. The GPS-based orbit solutions are determined in 30-h arcs that overlap by 6 h. The RMS radial orbit difference is computed for each 6-h overlap time period for all arcs ranging from cycle 8 through 24. Figure 3b shows a histogram of the radial orbit overlap difference RMS. It indicates the precision of the GPS RD solutions is at the 4-mm level.

TABLE 6 Orbit Difference Statistics Computed Per Cycle and Summarized Over Cycles 8–24

Solutions differenced	Avg. radial RMS (cm)	Avg. 3D RMS (cm)	Avg./Stdev of RSS[mean XY] per cycle (cm)	Avg./Stdev of mean Z per cycle (cm)
GPS RD—SLR+DORIS Dyn	1.365	6.053	0.479/0.586	0.071/0.362
GPS RD—SLR+DORIS RD	1.141	4.809	0.376/0.437	0.069/0.380
GPS RD—SLR+DORIS+ Xover RD	1.063	5.375	0.412/0.425	0.109/0.500
GPS RD—GPS+SLR RD	0.405	1.226	0.067/0.125	0.075/0.119
SLR+DORIS+Xover RD—SLR+DORIS Dyn.	0.946	5.396	0.591/0.271	−0.044/0.299

Again, this is only a measure of radial orbit precision, but is a necessary condition for meeting the 1-cm goal and represents the POD accuracy limit. The tracking data residual analysis presented above, and in particular the high elevation SLR analysis results, indicate the GPS RD and GPS+SLR RD radial orbit accuracy is likely meeting the 1-cm goal.

Independent Solution Orbit Difference Analysis

Another useful means of characterizing orbit error is to compare ephemerides computed from independent tracking data and solution techniques. Comparing orbits computed from independent tracking data can reveal systematic errors, especially measurement modeling errors. When comparing orbits computed from dynamic and reduced dynamic techniques, force modeling errors in the dynamic orbit and measurement modeling errors in the reduced dynamic orbit can be revealed (Christensen et al. 1994; Marshall et al. 1995). A summary of our orbit difference analysis is presented in Table 6. Orbit differences are computed for each 10-day arc comprising a repeat cycle, and the statistics are averaged over cycles 8–24. The first three rows of Table 6 present the summary of various SLR+DORIS based orbits differenced with the GPS RD orbits (our best performing solutions). The results show improved radial agreement is achieved by employing the reduced dynamic technique in the SLR+DORIS-based solutions. Still further radial agreement is achieved by including altimeter crossover data in the SLR+DORIS RD solution. The results show it is possible to obtain 1-cm radial RMS orbit agreement between solutions computed from two independent sets of tracking data. This demonstrates that we have achieved good consistency in measurement modeling and well tuned solutions. Additionally, this is a further indication that our orbits likely achieve the 1-cm goal. Also shown in Table 6 are the summary statistics for GPS RD—GPS+SLR RD orbit differences. In this case a 4-mm radial RMS orbit difference is observed. As expected, this is in excellent agreement with the 4-mm radial RMS orbit improvement predicted by the crossover residual analysis presented above.

Force modeling errors, such as mean geographically correlated gravity error, and measurement modeling errors, such as realizations of the Terrestrial Reference Frame (TRF), can impart mean offsets in the ECF frame which can then adversely affect altimeter derived estimates of sea surface topography (Marshall et al. 1995; Christensen et al. 1994; Rosborough et al. 1986). The anticorrelated gravity error is dependent on the satellite motion and causes an equal magnitude but opposite sign radial orbit error between ascending and descending orbit tracks (Marshall et al. 1995; Rosborough et al. 1986). The anticorrelated gravity error remains constant for each orbit repeat cycle and will impact altimeter

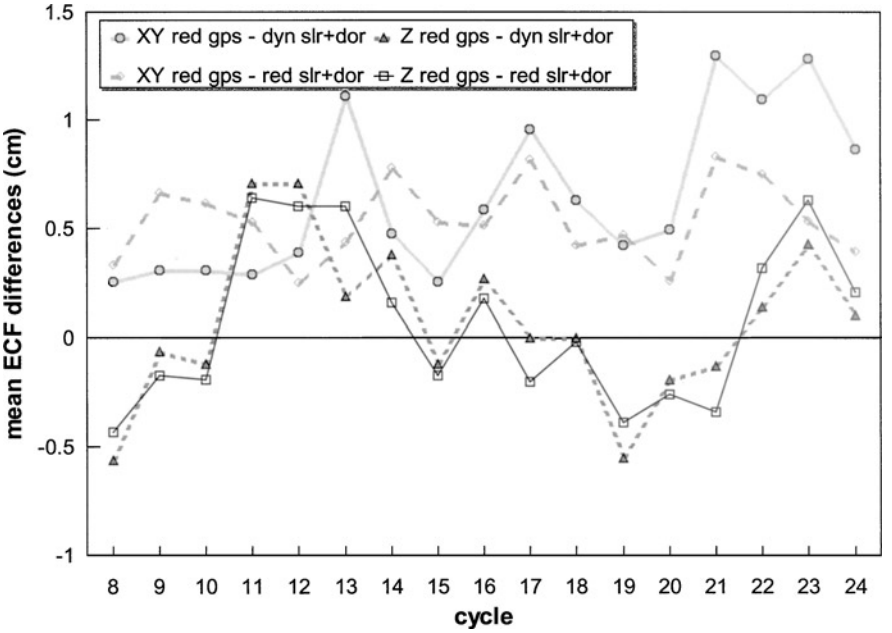

FIGURE 4 Mean orbit differences. The figure shows orbit consistency by cycle in the ECF equatorial (XY) plane, and about the Z axis between the GPS reduced dynamic and SLR+DORIS solutions. The better comparison between the reduced-dynamic solutions suggests orbit consistency in the equatorial plane depends on force modeling accuracy, namely the geographically correlated gravity error. The orbit consistency about Z, is largely determined by reference system consistency. The dynamic SLR+DORIS orbit has traditionally served to monitor orbit consistency along the Z axis with an expected resolution of 5–6 mm. These orbits show a Z RMS of 4 mm, with an apparent 120-day period.

crossover analysis of sea surface variability. Orbit difference tests can be used to observe the mean geographically correlated errors.

For each cycle we have computed the mean orbit difference in the equatorial plane (RSS of the ECF X and Y mean) and in the Z direction. Table 6 shows the average of these statistics over cycles 8–24. The average and variation of the mean equatorial offset between GPS RD and SLR+DORIS-based solutions has been decreased when the reduced dynamic technique is used in the SLR+DORIS-based solution (Figure 4). Therefore, the reduced dynamic technique can be successfully applied in a SLR+DORIS solution to accommodate the known mean geographically correlated gravity error remaining in the JGM3 gravity model (Marshall et al. 1995). The SLR+DORIS+Xover RD solutions show larger mean offsets from the GPS RD solution than does the SLR+DORIS RD solution. It is important to note that the crossover data contains additional error sources such as altimeter noise, altimeter correction error, and variations in the sea surface topography. The largest mean equatorial offset is found in the difference between SLR+DORIS+Xover RD and the SLR+DORIS Dyn, where both mean geographically correlated error and altimeter measurement modeling errors corrupt the orbit solutions in this comparison.

When a reduced dynamic technique is employed in the SLR+DORIS-based solutions, the average of the mean ECF offsets in the equatorial plane between these solutions and the GPS RD solutions is better than 4.0 mm. This is due to the significant reduction in mean geographically correlated gravity error obtained by applying the reduced dynamic technique

to the SLR+DORIS solutions. It is also important to note that the variation of the mean equatorial offset from cycle to cycle has a standard deviation of 4.4 mm and no significant outliers (Figure 4). These remaining equatorial plane offsets are the result of remaining geographically correlated error (limited by the SLR+DORIS RD) and possibly reference frame errors leaking into the reduced dynamic solutions. In the Z direction, the average of the mean ECF offset is at the 1-mm level with standard deviation of less than 4 mm and a $\sim$120-day periodicity. Employing a reduced dynamic technique in the SLR+DORIS solution does not reduce the average and variation of the mean Z offset, nor does it reduce the periodic structure (Figure 4). Still, this level of agreement in the Zoffset is quite good and represents a significant improvement over that found with T/P POD analysis (Marshall et al. 1995). At this current level of agreement it is not clear whether the SLR+DORIS or the GPS-based orbits are dominating the remaining Z difference signal. The dynamic SLR+DORIS orbit solution has traditionally served to monitor orbit consistency along the Z axis with an expected resolution of 5–6 mm. However, this analysis shows we can no longer assume the SLR+DORIS-based orbit solutions are the best centered. The GPS-based orbits also show the least variation of the crossover residual means (Table 5), another metric of orbit consistency. The improvement in the GPS-based RD solutions can be attributed to significant improvements in the consistency of ITRF2000 station positions across tracking technologies, and also to a lesser extent improvements in the Jason-1 GPS space receiver, GPS satellite orbits, GPS measurement modeling (e.g., GPS attitude, tracking offsets, APC map), and processing tools and techniques.

In addition to the statistics presented in Table 6, Figure 5 presents a view of the geographically correlated radial orbit error by computing the mean (Figure 5a and 5b) and standard deviation about the mean (Figure 5c and 5d) of the radial orbit differences in $5^\circ \times 5^\circ$ bins. Figures 5a and 5b show the geographically correlated orbit error is significantly reduced in overall power (from 4.8 mm to 3.4 mm) and structure. This is the reduction in the JGM3 mean geographically correlated gravity error achieved by using a reduced dynamic technique in the SLR+DORIS-based solutions. Figures 5c and 5d also show a reduction in the power and structure of the standard deviation of the mean when employing the reduced dynamic technique to SLR+DORIS-based solutions. In addition to accounting for geographically correlated gravity error, the reduced dynamic technique is accounting for anticorrelated gravity error and time varying error caused by tidal and nonconservative force model errors. However, this analysis is not limited to characterizing the improvement over SLR+DORIS Dyn solutions obtained by the SLR+DORIS RD and GPS RD solutions.

The analysis also gives a glimpse of the orbit error remaining in our best solutions (Figures 5b and 5d). As we have shown (Figure 5a and 5c), using orbit differences between SLR+DORIS Dyn and GPS RD largely serves to characterize the orbit error in the inferior SLR+DORIS Dyn solution arising from errors in the potential and nonconservative force models. In order to characterize the orbit error remaining in our GPS RD solutions we needed an orbit solution computed from independent tracking data that provides as close as possible overall performance. Our SLR+DORIS+Xover RD orbits, which have been shown to be our best-performing orbits computed without GPS data, served as our comparison solution (Figure 5b and 5d). Still the results shown in Figure 5b and 5d are likely dominated by the errors in the SLR+DORIS+Xover RD solution and should be viewed as an upper bound for our GPS RD and GPS+SLR RD solutions. Although not shown in a figure here, the spectrum of the radial orbit difference between GPS RD and SLR+DORIS Dyn solutions is as expected with the dominant power at 1-cpr and modulations of the 1-cpr by 1, 2, and 3 cycles per day (cpd) terms caused by nonconservative force modeling error, gravity error, and reference frame error (Marshall et al. 1995). As expected, a similar structure, but containing less power, is seen in the GPS RD and SLR+DORIS+Xover

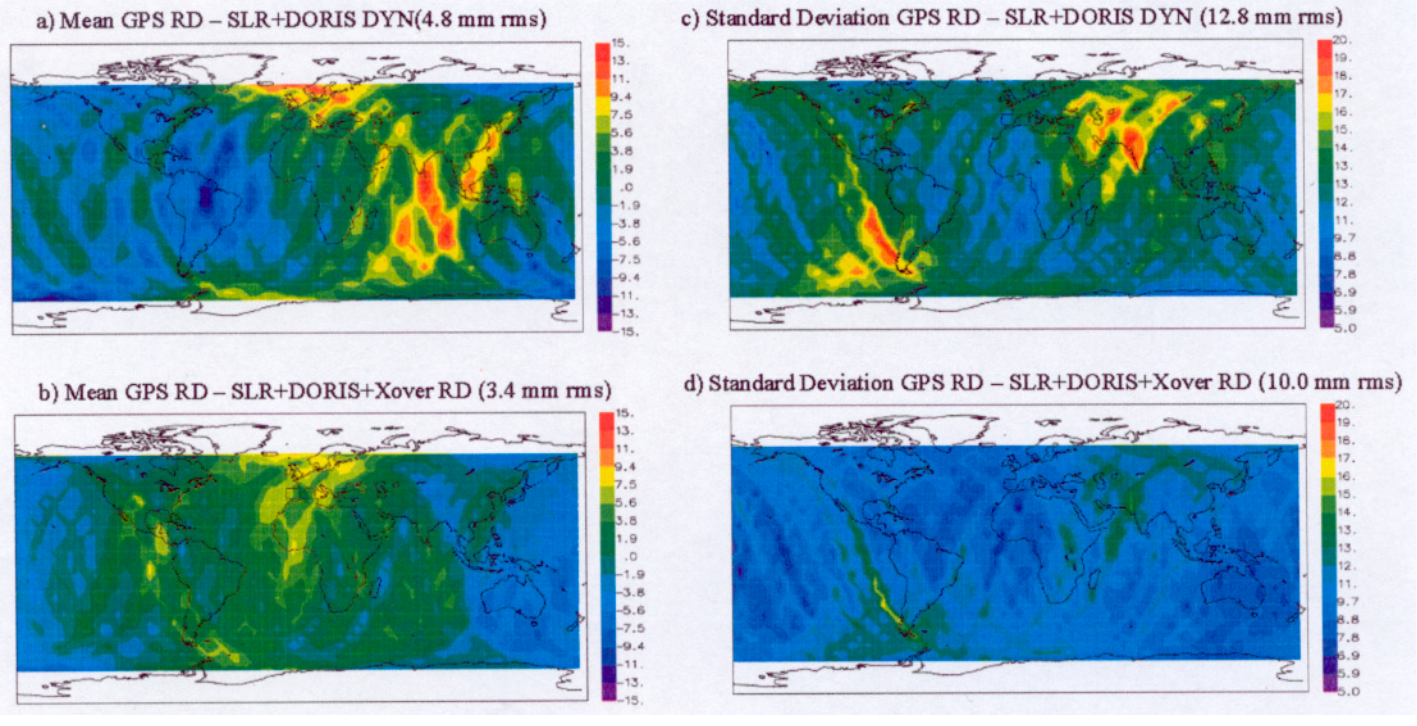

FIGURE 5 Radial orbit difference maps. GPS reduced-dynamic radial orbit differences averaged over $5^\circ \times 5^\circ$ bins for cycles 8–24, show that the geographically correlated gravity error of about 5 mm observed in the SLR+DORIS dynamic solutions is significantly diminished in the SLR+DORIS+Xover reduced-dynamic orbit comparison (a) and (b). The figures show the geographically correlated gravity error is significantly decreased when using the reduced dynamic technique even in a solution not computed from GPS data. The reduction in the standard deviation about the mean shown between the same two sets of orbit differences indicates the significant removal of geographically anticorrelated gravity error and possibly tide and nonconservative force modeling error when using the reduced-dynamic technique (c) and (d). (b) and (d) give a glimpse of the geographically correlated errors remaining in our best solutions. Although, the errors are dominated by the SLR+DORIS+Xover reduced dynamic solution, and therefore, the GPS-based reduced dynamic solutions actually have smaller errors.

RD orbit difference spectrum because the reduced dynamic technique accounts for more of the modeling errors.

Recovered Empirical Acceleration Analysis

The previous tracking data residual and orbit difference analysis demonstrates the reduced dynamic solution technique significantly improves radial orbit accuracy in an overall sense and reduces geographically correlated structure arising from gravity errors. However, it is important to understand whether the recovered accelerations actually represent physical phenomena in order to lend more confidence to the reduced dynamic technique. Figure 6a

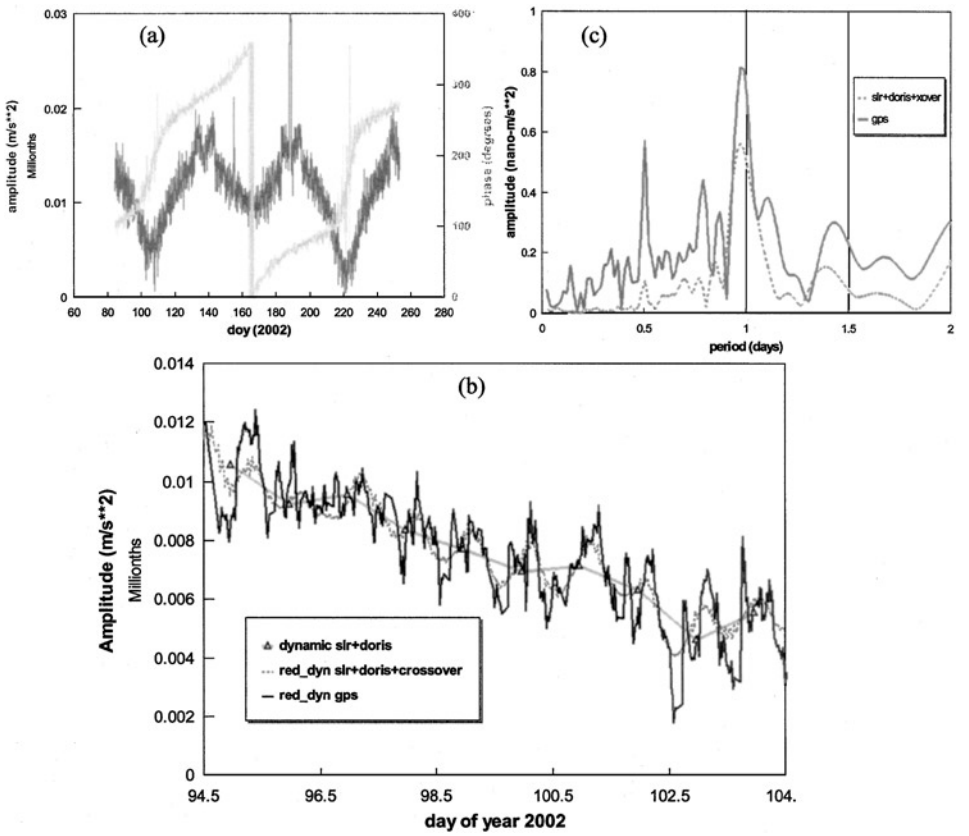

FIGURE 6 Recovered along-track 1-cpr accelerations, (a) The 1-cpr along track acceleration amplitude and phase adjusted over 30-min spans from each of the GPS reduced-dynamic 30-h arcs demonstrate a remarkably coherent large scale correlation with β'. (b) The along-track 1-cpr acceleration amplitude adjusted over cycle 9 for three solutions: SLR+DORIS dynamic, SLR+DORIS+Crossover reduced dynamic, and GPS reduced dynamic are compared. There is a striking similarity in the accelerations captured from completely different tracking technologies using the reduced dynamic technique. (c) Spectral analysis of the 1-cpr along-track acceleration amplitudes from reduced-dynamic solutions. Although both display similar structure, considerably more power is captured in the GPS RD solution at many main frequencies. These figures demonstrate the capability of the reduced-dynamic approach to compensate for mismodeled forces where the GPS RD solution offers the best resolution for representing the mismodeled forces.

presents the recovered amplitude and phase of the along track 1-cpr accelerations adjusted in 30-min time spans from each of the GPS RD 30-h arcs spanning nearly 1.5 cycles in β' (angle between the Earth-Sun Vector and the orbit plane). The figure shows a remarkably coherent large-scale correlation with β' and demonstrates the capability of the reduced dynamic approach to compensate for mismodeled forces, dominated in this case by radiation pressure. Figure 6b shows the recovered amplitude of the 1-cpr along-track accelerations estimated over cycle 9 using three different solutions: SLR+DORIS Dyn, SLR+DORIS+Xover RD, and GPS RD. The figure shows the more frequent estimation of acceleration parameters used in the two solutions employing the reduced dynamic technique capture significantly more structure about the mean accelerations recovered in the dynamic solution. Although the GPS RD solution has more structure than the SLR+DORIS+Xover RD solution, there is a remarkable similarity in the accelerations captured from completely different tracking technologies using the reduced dynamic solution strategy. Figure 6c presents a periodogram of the recovered along-track 1-cpr acceleration amplitude for both the GPS RD and the SLR+DORIS+Xover RD solutions. Figure 6c gives another demonstration that different tracking technologies have captured a similar acceleration pattern. Although, both display similar structure, considerably more power is captured in the GPS RD solution at many main frequencies, demonstrating the GPS RD solution offers the best resolution for representing the mismodeled forces. The analysis shows the recovered accelerations from our reduced dynamic solution technique are physically realistic and compensate for gravity, tide, and nonconservative force model error, and therefore significantly improve the orbit accuracy as demonstrated in the previous analyses.

Crossover Residual Analysis

Long-period geographically correlated radial orbit error can mask and contaminate oceanographic signals observed through altimeter observations. Orbit errors arising from such sources as anticorrelated gravity error, tidal modeling error, and inertial reference frame errors can be a particular nuisance. In order to characterize these types of orbit errors we can exploit the altimeter crossover data itself beyond that discussed in the section on Tracking Data Residual and Orbit Overlap Analysis. Unlike orbit difference analysis, crossovers offer an important independent measure of orbit error such as the anticorrelated gravity error (Rosborough et al. 1986; Scharoo and Visser 1998). Figure 7 shows altimeter crossover residuals from cycles 8–24 averaged over $5^\circ \times 5^\circ$ bins for three different types of orbit solutions. The three maps show a progressive and significant reduction of the radial orbit error from the SLR+DORIS Dyn, to the SLR+DORIS+Xover RD, to the GPS RD solution. These maps show a good agreement to the orbit difference standard deviation maps shown in Figures 5c and 5d. It should be noted that the crossover data contain nonorbit signal including altimeter measurement error and oceanographic signal. Therefore, caution should be exercised when interpreting these results as an absolute measure of radial orbit error. Nevertheless, this analysis can be used as a relative gauge of orbit error and clearly demonstrates the GPS RD solutions are accommodating a significant part of the JGM3 anticorrelated gravity error. Although the crossover variance is dominated by oceanographic signal and altimeter modeling error, we have also observed a significant reduction in crossover variance using the GPS RD solution, as previously shown in Table 5. These crossover analysis results show a substantial improvement in radial orbit accuracy has been achieved by the GPS-based RD solutions accommodating gravity, tide and nonconservative force modeling errors.

The crossover residual mean computed globally per cycle allows us to observe anticorrelated gravity error and long period radial orbit error arising from such sources as tidal

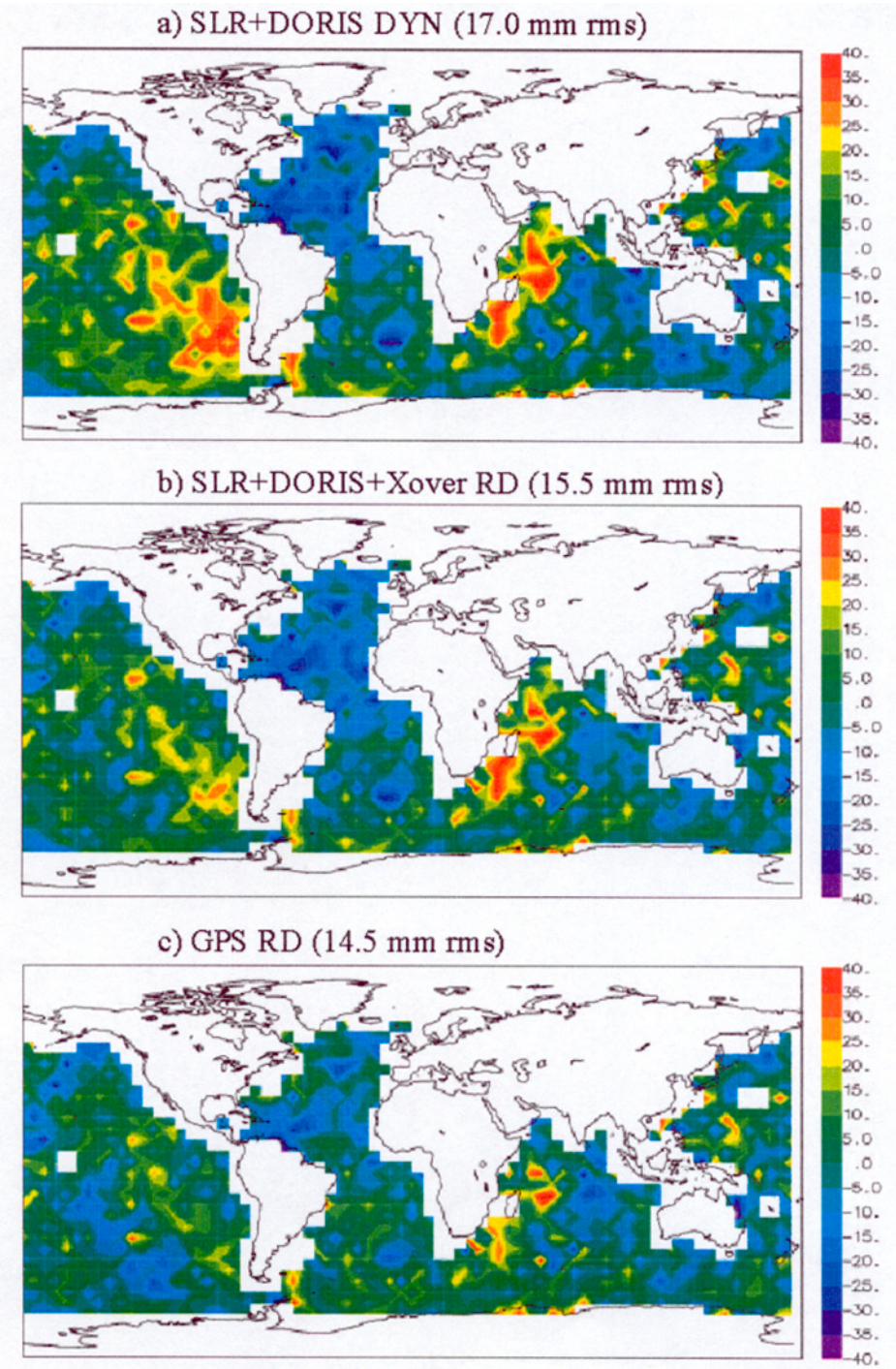

FIGURE 7 Average altimeter crossover residuals map. Crossover residuals averaged over $5^\circ \times 5^\circ$ bins for cycles 8–24 show radial orbit error primarily due to anticorrelated gravity error. The three maps show a progressive and significant reduction of this error from the dynamic SLR+DORIS to the reduced dynamic GPS solutions. These maps bare a good resemblance to the orbit difference standard deviation maps (Figures 6c and 6d). Unlike orbit differences, crossovers offer an independent direct measure of orbit error but also contain nonorbit signal.

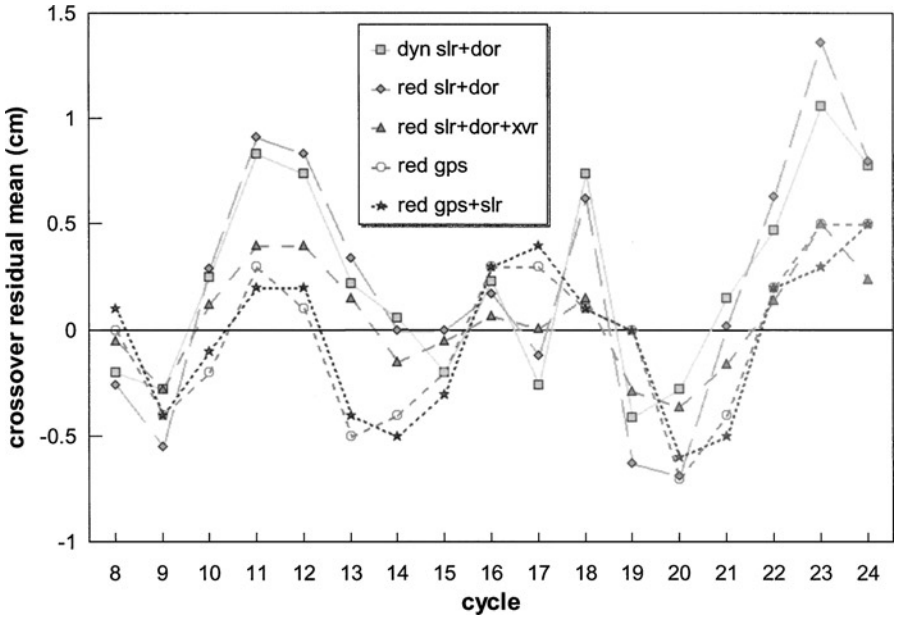

FIGURE 8 Crossover residual mean time series. Altimeter crossover residual means, cycles 8–24, show that the least variation are seen in the SLR+DORIS+Crossover, and GPS-based orbits. The most variation is seen with the SLR+DORIS orbits. The interesting, approximately 60-day signature, seen with all of the orbits and best seen with the GPS, may be due to a nonorbit effect such as mismodeling of surface tides, ionosphere or atmospheric pressure corrections.

modeling error and mean offsets in the inertial frame. Figure 8 presents a time series of altimeter crossover means computed globally per cycle. Of the solutions that are independent to the altimeter crossover data, the SLR+DORIS Dyn and RD solutions show a much larger variation and mean than the GPS-based RD orbits. Of particular interest in Figure 8 is the 60-day signature in the mean altimeter crossover residual time series clearly observed by the GPS-based orbit solutions. Orbit solutions based on SLR+DORIS data also see this 60-day signature but are much noisier or have an additional signal superimposed. The data in Figure 8 also show that employing the reduced dynamic technique in the SLR+DORIS-based solution does not significantly change this signal, lending input to the notion that this signal is not likely a force modeling error. Furthermore, because this signal is observed in both SLR+DORIS- and GPS-based solutions, and because of its 60-day periodicity, it is not likely due to mean offsets of the orbit in the inertial frame.

It is quite possible that this signal is not an orbit error at all, but arises from an altimeter measurement modeling error such as surface tide, ionosphere, or atmospheric pressure corrections. One possible explanation is that this error is caused by errors in the S2 and/or M2 constituents of the surface tide model used in the altimeter measurement modeling. The S2 and M2 tides have Jason-1 aliasing periods near 60 days and comprise two of the largest tidal constituents on the ocean surface (Marshall et al. 1995). The estimates of these tidal constituents could have been contaminated from errors in the T/P orbits that were computed based on SLR+DORIS Dyn solutions. We have seen throughout this article that these orbit solutions have significant force modeling errors. Therefore, it is possible that tidal, gravity, and nonconservative force modeling orbit errors could have corrupted the T/P-derived surface tide models at the dominant S2 and M2 constituents. It is possible that

we are now observing these tide modeling errors in the altimeter data itself because we have significantly reduced the orbit force modeling errors for Jason-1 using the GPS-based RD solution. However, further analysis will be necessary to fully understand this signal. Of course, this is one possible explanation, but the real importance of this analysis is that it shows the significant improvement in orbit accuracy achieved with the GPS-based RD solutions is now making it possible to observe altimeter measurement modeling errors and signal at the sub-cm level.

Conclusions

Achieving the Jason-1 radial orbit accuracy goal of 1-cm presented not only the challenge of producing these orbits, but also the challenge of demonstrating the accuracy of these orbits. Proper assessment of orbit accuracy, determination of the best orbit strategy, and characterization of the resultant orbit errors were the main goals of this article. Meeting these goals required the processing of all tracking data types available whether they were included in the orbit solution or withheld as independent data to assess orbit performance. We have computed and assessed the performance of five candidate orbit solutions determined from various combinations of the available Jason-1 tracking data and using different solution techniques. Using independent and dependent tracking data analysis, orbit difference analysis, and crossover residual performance analysis, we have demonstrated our GPS-based reduced dynamic orbits are achieving the 1-cm radial orbit accuracy goal. We have also demonstrated these orbits are very well centered and argued that the GPS-based orbits are as well centered or better than the SLR+DORIS orbits.

Towards the development and analysis of our orbits at the 1-cm level we have also produced significantly better orbits without GPS data. Specifically, the SLR+DORIS+XOVER RD orbits represent a significant improvement over the traditional SLR+DORIS Dyn orbits and provide the necessary independent high-accuracy orbits that compare at the 1-cm radial RMS level with our GPS-based reduced dynamic orbits. We have also demonstrated that combination GPS+SLR solutions outperform GPS-only solutions. Analysis of the time series of the crossover residual global mean computed per cycle shows the GPS reduced dynamic solutions clearly resolve a striking 60-day periodicity. It was hypothesized that the cause of this signal is likely error in the surface tide, ionosphere, and/or atmospheric pressure corrections in the altimeter measurement model and not an orbit artifact. The important point is that the GPS-based reduced dynamic orbits are now at the accuracy level that they can begin to resolve these types of signals.

The accuracy achieved by the GPS-based reduced dynamic orbits are a direct result of both hardware and reference frame improvements (stations and GPS orbits) and the many improvements made in the GPS measurement modeling, including the postlaunch determination of an antenna phase correction map. Further improvements in GPS tracking data such as cycle slip and noise reduction and further enhancements in measurement modeling such as integer ambiguity bias resolution and enhancements to the GPS station positions/orbits can further improve orbit accuracy. It is important to recognize that the SLR data provides an invaluable direct and independent measure of radial orbit accuracy for calibrating and validating our GPS-based solutions and has also been shown to improve upon these solutions when included in the orbit determination. Further orbit accuracy improvement can be realized by enhancements in the spatial and temporal distribution of the SLR tracking data. Nevertheless, the 1-cm orbit accuracy currently achieved by the GPS and GPS+SLR reduced dynamic solutions represents a significant improvement in radial orbit accuracy and will enable the resolution of new signals and features within the altimetry data.

References

Altamimi, Z., P. Sillard, and C. Boucher. 2002. ITRF2000: A new release of the International Terrestrial Reference Frame for earth science applications. *J. Geophys. Res.* 107(B10):ETG–1–19.

Bar-Sever, Y. E. 1996. A new model for GPS yaw attitude. *J. Geod.* 70:714–723.

Bertiger, W. I., Y. E. Bar-Sever, E. J. Christensen, E. S. Davis, J. R. Guinn, B. J. Haines, R. W. Ibanez-Meier, J. R Jee, S. M. Lichten, W. G. Melbourne, R. J. Muellerschoen, R. N. Munson, Y. Vigue, S. C. Wu, T. P. Yunck, B. E. Schutz, P. A. M. Abusali, H. J. Rim, M. M. Watkins, and P. Willis. 1994. GPS Precise Tracking of TOPEX/POSEIDON: Results and implications. *J. Geophys. Res.* 99(12):24449–24464.

Chelton, D. B., J. C. Ries, B. J. Haines, L.-L. Fu, and P. S. Callahan. 2001. Satellite Altimetry. pp. 64–68 in *Satellite altimetry and earth sciences: A handbook of techniques and applications*, L.-L. Fu and A. Cazenave, Eds. San Diego, CA: Academic Press.

Christensen, E. J., B. J. Haines, and K. C. McColl. 1994. Observations of geographically correlated orbit errors for TOPEX/Poseidon using the global positioning system. *Geophys. Res. Lett.* 21(19):2175–2178.

Colombo, O. L. 1989. The dynamics of Global Positioning System orbits and the determination of precise ephemerides. *J. Geophys. Res.* 94(B7):9167–9182.

Haines, B., W. Bertiger, S. Desai, D. Kuang, T. Munson, L. Young, and P. Willis. 2003a. Initial orbit determination results for Jason-1: Towards a 1-cm orbit. *J. Navig.* In press.

Haines, B., S. Desai, P. Willis, and W. Bertiger. 2003b. Precise orbit determination for Jason-1: GPS and the 1-cm challenge. *Geophys. Res. Abst.* 5:12378.

Hedin, A. E. 1988. The atmosphere model in the region 90 to 200 km, *Adv. Space Res*. 8(5):9-25.

Marshall, J. A., N. P. Zelensky, S. B. Luthcke, K. E. Rachlin, and R. G. Williamson. 1995. The temporal and spatial characteristics of TOPEX/Poseidon radial orbit error. *J. Geophys. Res.* 100(C12):25331–25352.

Ray, R. D. 1999. A global ocean tide model from TOPEX/POSEIDON altimetry: GOT99.2, NASA/TM-1999-209478, GSFC.

Rosborough, G. W. 1986. Satellite orbit perturbations due to the Geopotential, Ph.D. dissertation, Center for Space Research, The University of Texas at Austin.

Rowlands D. D., S. B. Luthcke, J. A. Marshall, C. M. Cox, R. G. Williamson, and S. C. Rowton. 1997. Space shuttle precision orbit determination in support of SLA-1 using TDRSS and GPS tracking data. *J. Astronaut. Sci.* 45(1):113–129.

Scharroo, R., and P. N. A. M Visser. 1998. Precise orbit determination and gravity field improvement for the ERS satellites. *J. Geophys. Res.* 103:8113–8127.

Tapley, B. D., J. C. Ries, G. W. Davis, R. J. Eanes, B. E. Schutz, C. K. Shum, M. M. Watkins, J. A. Marshall, R. S. Nerem, B. H. Putney, S. M. Klosko, S. B. Luthcke, D. E. Pavlis, R. G. Williamson, and N. P. Zelensky. 1994. Precision orbit determination for TOPEX/Poseidon. *J. Geophys. Res.* 99(12):24383–24404.

Tapley, B. D., M. M. Watkins, J. C. Ries, G. W. Davis, R. J. Eanes, S. R. Poole, H. J. Rim, B. E. Schutz, C. K. Shum, R. S. Nerem, F. J. Lerch, J. A. Marshall, S. M. Klosko, N. K. Pavlis, and R. G. Williamson. 1996. The JGM-3 geopotential model. *J. Geophys. Res.* 101:28029–28049.

Willis, P., B. Haines, Y. Bar-Sever, W. Bertiger, R. Muellerschoen, D. Kuang, and S. Desai. 2003. TOPEX/JASON combined GPS/DORIS orbit determination in the tandem phase. *Adv. Space Res.* In press.

Yunck, T. P., W. I. Bertiger, S. C. Wu, Y. E. Bar-Sever, E. J. Christensen, B. J. Haines, S. M. Lichten, R. J. Muellerschoen, Y. Vigue, and P. Willis. 1994. First assessment of GPS-based reduced dynamic orbit determination on TOPEX/Poseidon. *Geophys. Res. Lett.* 21(7):541–544.